APL Materials

A nanoscale analysis method to reveal oxygen exchange between environment, oxide, and electrodes in ReRAM devices

Cite as: APL Mater. **9**, 111109 (2021); https://doi.org/10.1063/5.0070046
Submitted: 03 September 2021 • Accepted: 24 October 2021 • Published Online: 09 November 2021

Horatio R. J. Cox, Mark Buckwell, Wing H. Ng, et al.

A nanoscale analysis method to reveal oxygen exchange between environment, oxide, and electrodes in ReRAM devices

Cite as: APL Mater. 9, 111109 (2021); doi: 10.1063/5.0070046
Submitted: 3 September 2021 • Accepted: 24 October 2021 •
Published Online: 9 November 2021

Horatio R. J. Cox,[1,a] Mark Buckwell,[2] Wing H. Ng,[1] Daniel J. Mannion,[1] Adnan Mehonic,[1] Paul R. Shearing,[2] Sarah Fearn,[3] and Anthony J. Kenyon[1,b]

AFFILIATIONS

[1] Department of Electronic and Electrical Engineering, University College London, Torrington Place, London WC1E 7JE, United Kingdom
[2] Department of Chemical Engineering, University College London, Torrington Place, London WC1E 7JE, United Kingdom
[3] Department of Materials, Imperial College London, South Kensington Campus, London SW7 2AZ, United Kingdom

Note: This paper is part of the Special Topic on Materials Challenges for Nonvolatile Memory.
[a] **Author to whom correspondence should be addressed:** horatio.cox.17@ucl.ac.uk
[b] **E-mail:** t.kenyon@ucl.ac.uk

ABSTRACT

The limited sensitivity of existing analysis techniques at the nanometer scale makes it challenging to systematically examine the complex interactions in redox-based resistive random access memory (ReRAM) devices. To test models of oxygen movement in ReRAM devices beyond what has previously been possible, we present a new nanoscale analysis method. Harnessing the power of secondary ion mass spectrometry, the most sensitive surface analysis technique, for the first time, we observe the movement of ^{16}O across electrically biased SiO_x ReRAM stacks. We can therefore measure bulk concentration changes in a continuous profile with unprecedented sensitivity. This reveals the nanoscale details of the reversible field-driven exchange of oxygen across the ReRAM stack. Both the reservoir-like behavior of a Mo electrode and the injection of oxygen into the surface of SiO_x from the ambient are observed within one profile. The injection of oxygen is controllable through changing the porosity of the SiO_x layer. Modeling of the electric fields in the ReRAM stacks is carried out which, for the first time, uses real measurements of both the interface roughness and electrode porosity. This supports our findings helping to explain how and where oxygen from ambient moisture enters devices during operation.

I. INTRODUCTION

Redox-based resistive random access memory (ReRAM) has been extensively studied over the last decade for the next generation of non-volatile memories and novel neuromorphic, brain-inspired, electronic technologies. Using Resistance Switching (RS) (or ReRAM) devices as "synapses" is a promising route to neuromorphic systems due to their two-terminal structure, stability (>10 years retention), high endurance (>10^{12} cycles), and multi-level analog states.[1–3] Although many types exist, in this work the focus is on "intrinsic" resistance switching devices, comprising a high resistance thin oxide (>$10^7\Omega$) sandwiched between two electrodes.[4] Intrinsic switching relies on changing the properties of the pure oxide without any indiffusion of conductive species from the electrodes. As the oxide is only nanometers thick, a small voltage applied between the electrodes generates large enough electric fields to drive oxygen diffusion. This initially lowers the resistance of the device—an effect currently attributed to conductive oxygen vacancy filaments forming between the electrodes. Subsequent voltage pulses sequentially break and reform these filaments through redox processes, allowing information to be stored in the changing device resistance.

However, the reliability of ReRAM technology is still a pressing issue. Seemingly identical devices behave differently, with no clear explanation why. Recent work has shown that during operation the

devices interact with the ambient environment. The voltage required to change the resistance of a device varies depending on the moisture content of its surroundings.[5,6] This provides one possible source of the unexplained repeatability issues in device performance. Finding a solution to this is proving difficult as our understanding of the ionic diffusion at the heart of ReRAM operation is largely theoretical. Collecting empirical measurements of nanoscale changes occurring in ReRAM devices is challenging and is the greatest obstacle to their development.[7] At present, it is unclear exactly how and where interaction with the ambient occurs. Indeed, direct experimental evidence, even for oxygen movement within the oxide layer itself, is limited. Most literature does not provide evidence for chemical changes during stress—they are inferred. This is with good reason, as measuring the small fluctuations in oxygen stoichiometry responsible for changes in conductivity pushes the limits of even state-of-the-art instrumentation. These interactions occur on the nanoscale, in an oxide matrix with an abundance of oxygen.

There has been a mixture of compositional and structural techniques used to study ReRAM devices. All have a trade-off between resolution, sensitivity, and measured sample volume. For example, Transmission Electron Microscopy (TEM) provides a wealth of structural information; combined with Electron Energy Loss Spectroscopy (EELS) and Energy Dispersive X-ray Spectroscopy (EDX), it excels at analyzing highly localized regions of significant chemical change surrounding conducting filaments.[8,9] However, it requires extensive sample preparation, measures a small fraction of the sample volume, and has limited sensitivity. We have previously shown that bulk changes—within the whole device volume, not just the filament—are crucial to device operation and require further investigation.[10] Hence, the interest here was to develop a complimentary method that could measure oxygen diffusion within the whole volume of the ReRAM stack. This requires an instrument capable of measuring a whole device with a nanoscale depth resolution. It also needs high sensitivity as the local changes in oxygen concentration are likely to be small.

Secondary Ion Mass Spectrometry (SIMS) is the most sensitive surface analysis technique and appears to be the best candidate for our purposes. It can measure changes in the chemical composition for large areas as a sample is depth profiled, with a resolution of a few atomic layers and a sensitivity of parts per billion.[11,12] As whole devices can be measured, oxidation and contamination are minimized so that analysis can be carried out after biasing devices in ambient moisture. However, there are major obstacles that have, until now, prevented SIMS from providing the level of detail required. First, instrumental variation, two sequential experiments on the same device, at the scale required, can return different results.[13] This makes it difficult to reliably measure small changes in the ion concentration between devices. Second, it is difficult to interpret and compare results due to charge transfer, which causes intensity enhancements at interfaces,[14] and matrix effects: The measured ion signals are not linearly proportional to their concentration but also dependent on the surrounding material.[11] Both factors mean that the measured oxygen signal could change through a material in which the concentration of oxygen remains constant. Consequently, ReRAM research has only used SIMS to measure average changes in oxide stoichiometries,[15] metal diffusion,[16,17] or isotope tracer concentrations.[18] So far, it has not been used to properly test models for oxygen movement within the device because, until now, it has not been possible to do so. This is illustrated in the work of Heisig *et al.* in which ReRAM devices were cycled in an $H_2{}^{18}O$ enriched atmosphere. Using SIMS depth profiling, ^{18}O was seen to diffuse into the device during operation, but it was not possible to detect a significant difference in the ^{16}O profile of pristine and cycled devices.[18]

Here, we present a procedure that mitigates these limitations—repeatability, charge transfer, and matrix effects. The key is *in situ* normalization, in which every electrically biased region is compared with a pristine (unbiased) region from the same analysis. We can isolate changes induced by biasing, reliably harnessing the sensitivity of SIMS to study small changes in ion concentrations through a stack of thin films. This enables us to start tackling several open questions: Where is the oxygen reservoir? What is the role of ambient oxygen in switching and how far into the structure does it penetrate? How dynamic are the interfaces under electrical stress? Below, we discuss the process of developing the procedure—describing chronologically each obstacle faced and the measures used to overcome them. Then, applying the procedure to several devices, we answer these questions, revealing new details in the process of oxygen exchange across ReRAM devices.

A. Measuring nanoscale changes

The first obstacle encountered was recoil implantation and cascade mixing: The top electrode obstructs the measurement of the switching layer. In SIMS, the layers of the sample are analyzed sequentially before being sputtered away, generating a depth profile. The sputtering and analysis ion beams can drive target atoms from the top electrode into the oxide. Recoil implantation occurs from direct collisions of the ion beam and material, cascade mixing from further secondary collisions. This causes contamination and can distort measurements.[11]

Here, we wanted to look across ambient–oxide–metal interfaces in several small, biased regions. In order to prevent ion beam mixing effects, rather than using a top electrode, bias was applied to the devices using a Conductive Atomic Force Microscopy (CAFM) tip scanned over the oxide, leaving an exposed oxide surface for analysis.[19] The aim was to induce field driven oxygen diffusion within the bulk of the oxide. Instead of measuring filaments, the interest was in how the broader bulk of the oxide would change under an electric field. Initially, the tip was held at a constant voltage as it scanned over the sample surface. However, it was found that this led to the complete breakdown of the oxide in regions within the scanning window, leaving the surface too damaged for further analysis. Therefore, the CAFM was operated in a constant-current mode, adjusting the voltage applied to the tip as it scanned to maintain a constant current, which prevented oxide breakdown. CAFM biasing of areas was carried out with target currents of 100 and 250 pA, while control areas were left pristine for comparison (Fig. 1). These target currents were not achieved due to the CAFM frequently reaching the maximum voltage it could apply (±10 V) and so being unable to induce any further increase in current. However, there were measurable differences in the average current and voltage applied to areas. Preliminary testing showed that there were distinct changes to the resistance of the oxide after CAFM biasing, an effect described in previous work.[20] Modeling, shown below, confirmed that this CAFM biasing

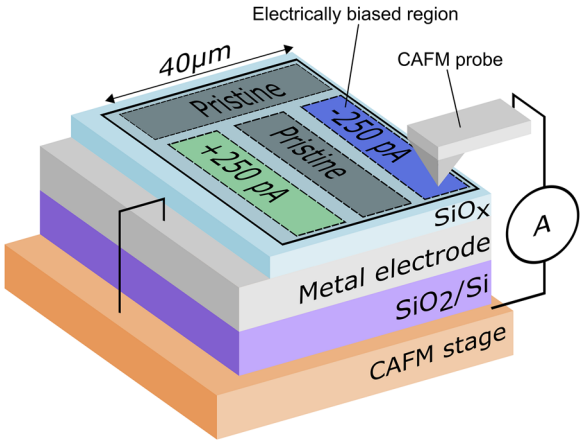

FIG. 1. Schematic of the CAFM experimental setup. The square outlined in black on SiO_x shows the scanning window used for the SIMS depth profiling. This window contains CAFM electrically biased regions used to measure changes during operation and pristine spanning strips used for calibration and normalization. The same setup was used for all the experiments in this work, but different metal electrodes were used in different samples: Ti, Mo, and Pt.

produced fields and interaction with the ambient comparable to those of a conventional top electrode.

The second, and perhaps biggest, challenge was extracting compositional information from the SIMS measurement. Due to matrix and charge transfer effects, the measured signal for each ion is not proportional to its concentration. It is instead a convolution of this and the sample chemistry in the region it is ejected from. The local environment of the atom being ejected determines the probability that it will ionize and therefore be measured. This is important because a very small proportion of ejected atoms are ionized and subsequently detected. For example, in silicon, typically ~0.1% of ejected dopant boron atoms are detected.[21] Hence, the amount of an element measured is strongly linked to how easily it is ionized. This is different for each element, in each material, at each distance from an interface.

This can be mitigated in the "dilute limit" regime for dopants of a very low concentration ($\ll$1%). Here, the dopants are too dilute to influence the chemistry of the system significantly. Comparing the results with reference samples, dopants or impurities can be measured quantitatively at a very low concentration in a carefully controlled environment.[22] However, this is not possible for our samples as oxygen is both abundant and mobile during operation. However, this strict quantitative approach is not necessary. What we are interested in is not measuring the exact chemistry of the system, but rather how the ions are moving, and their changing concentrations. By comparing each electrically biased region with a pristine untouched region, we have a reference, at each depth, for the oxygen signal from an undisturbed device. Carrying out point to point normalization between this pristine region and the biased regions allows us to compare the oxygen signal at each depth in the profile, countering the matrix and charge transfer effects. At each depth, these effects are approximately the same for the pristine and electrically biased areas. Hence, normalizing one to another minimizes any enhancements, isolating the changes in oxygen concentration across the device. This same principle, which makes SIMS powerful when looking at isotopic tracers, can extend to ions already present in the material. It should be noted that these results are semi-quantitative as oxygen changes in our devices were significant enough that the pristine and biased regions changed in composition enough to slightly alter the probability of ionization at each depth. Nevertheless, it is a powerful means of determining where and by how much the oxygen movement occurs. However, this normalization requires very reliable and reproducible experiments. Otherwise, differences in the measurements could shift the results making changes appear where they are not present. This brings us to our final obstacle, instrumental variation.

At present, SIMS is used to study changes induced during operation by separately measuring different devices. Between experiments, several parameters such as beam current, focus, and chamber pressure vary no matter how tightly one tries to control them. As a result, sequential experiments, even on identical devices, do not match precisely. Typically, without further processing, this variation limits the precision between experiments to around 10%.[13] This introduces an error into our measurement greater than the changes we were looking to measure. As an example, we measured the oxygen signal in SiO_x for two sequential runs in a pristine region. The two scans were done on the same device (a 12 nm thick sputtered SiO_x film on a titanium electrode) under identical instrumental conditions. For 60 data points, in a uniform region of SiO_x, the difference between these measurements has a mean and standard deviation of 16.7% and 6.4%, respectively. To measure changes of a few percent, we need to improve on this significantly.

The simple but effective solution is to measure all regions in one run. The measurement error then becomes the variation across the scanning window—which can be checked and calibrated using the perpendicular pristine strips spanning it (Fig. 1). These calibration strips were important as it was found that extremely careful control of the beam parameters and focus were required to prevent systematic shifts in ion counts—perhaps beyond those usually required. Carrying out the same comparison as above but instead between two regions from the same scan of one device, returns a mean and standard deviation in the difference between sequential measurements of 1.4% and 0.8%, respectively. This is almost an order of magnitude improvement in both.

Figure 2 shows a comparison between this new method of *in situ* normalization (blue) and conventional normalization (purple) for an oxygen depth profile of electrically biased regions. The full depth profile data are not plotted. Instead, it starts 7 nm into the oxide and focuses on the interface with the bottom electrode. The plot shows the change in oxygen concentration with depth, across the interface, from SiO_x into a titanium bottom electrode. The error in the conventional normalization would lead to the false conclusion that biasing reduces the oxygen concentration across the whole interface. The reduction in error for the *in situ* normalization shows that the biasing has driven oxygen across the interface and into the titanium electrode.

II. RESULTS AND DISCUSSION

Having confirmed that our experimental method allows us to reliably detect small changes in oxygen stoichiometry, we applied

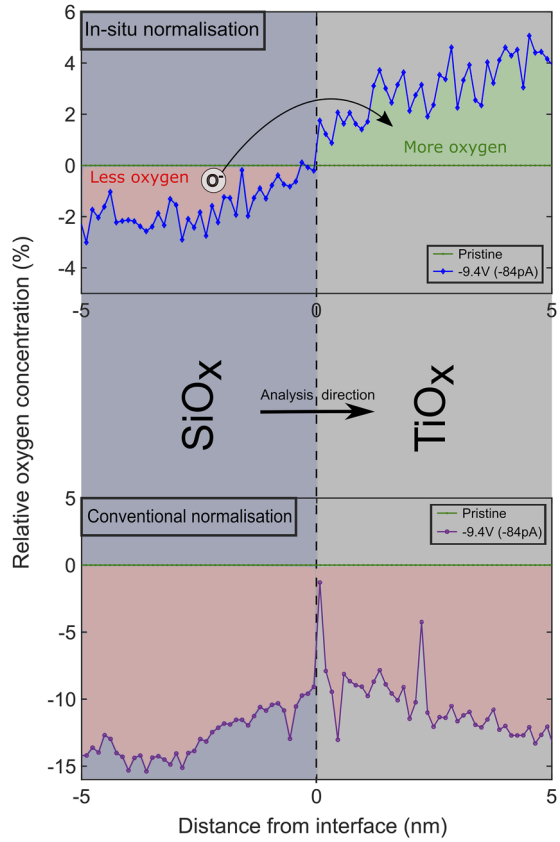

FIG. 2. Comparison of SIMS normalization methods measuring changes in the oxygen signal. The purple line (lower panel) shows the measured changes induced by biasing using conventional analysis, and the blue line (upper panel) shows the same after *in situ* normalization. The large errors in the conventional analysis mask the diffusion of the oxygen. *In situ* normalization reduces the error, revealing oxygen to have been driven across the interface from SiO_x into the Ti electrode. The measured average voltage and current applied to the area with the CAFM are displayed in the key. The Ti layer has been labeled an oxide (TiO_x) as a lot of oxygen was measured there. The depth scale is approximate in TiO_x as sputtering rates vary.

it to ReRAM devices. First, we looked at the interface between the SiO_x switching layer and bottom electrode. Although the changes in device resistance are believed to result from oxygen movement within the oxide itself, the electrode plays an important role as a reservoir. If the electrode can reversibly store and release oxygen from the oxide, it is likely to result in more stable devices. If instead the exchange of oxygen between the oxide and electrode is prevented, it can result in electrode delamination, oxygen loss from the system, and eventually device failure.[23] Szot *et al.* observed such delamination, with nanometer-sized bubbles of oxygen forming at an interface between $SrTiO_3$ and a platinum electrode after cycling.[24] We hypothesize that the reason for delamination is poor exchange of oxygen with the platinum electrode. Platinum does not typically form oxides, and so the oxygen expelled from $SrTiO_3$ is reduced, becoming gaseous and damaging the device. Using a metal electrode more readily able to accept oxygen should prevent this expulsion of oxygen at the interface. Our devices with molybdenum lower electrodes perform well.[25] We hypothesize that this is a result of molybdenum oxide and the SiO_x switching layer having Gibbs free energies of oxide formation, which are relatively close (SiO_2 = −856.3 kJ mol^{-1}, MoO_3 = −668.0 kJ mol^{-1}).[26] This might enable oxygen to be exchanged across the interface via redox reactions, preventing gas evolution. To test this hypothesis, we measured changes after biasing, depth profiling a device from the ambient through SiO_x (12 nm) and Mo (200 nm), as shown in Fig. 3. Under opposite biases, oxygen was driven in different directions across the SiO_x/Mo interface. This revealed the role of the molybdenum as an oxygen reservoir, an effect that has previously been measured for other materials systems.[28–30] When a negative tip bias was applied to the SiO_x surface, oxygen from SiO_x was stored through oxidation of the

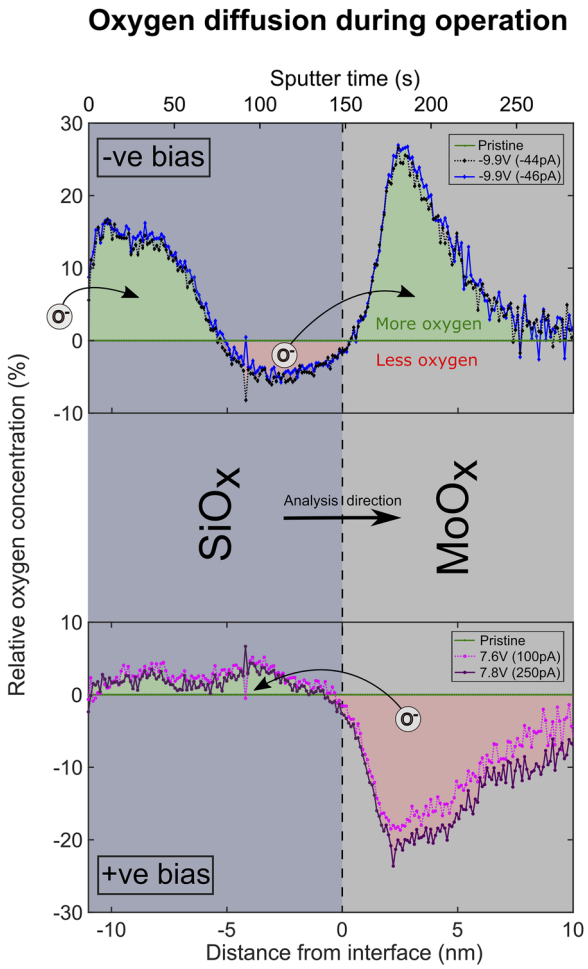

FIG. 3. Depth profile through a biased ReRAM device with negative (upper panel—blue/black) and positive (lower panel—pink/purple) voltages applied to the CAFM tip. The measured average voltages and currents applied to each area with the CAFM are displayed in the key. The plots have been normalized to a pristine region and thus show the changes in the oxygen concentration induced by biasing. The curved arrows show the direction of oxygen diffusion during biasing. The Mo layer has been labeled an oxide (MoO_x) as a lot of oxygen was measured there. The depth scale is approximate in MoO_x as sputtering rates vary.

molybdenum. When a positive tip bias was applied oxygen diffused into SiO_x through reduction of the molybdenum. There were relative oxygen concentration changes near the interface of approximately a few percent in SiO_x, which are not detectable without our *in situ* normalization.

The consistency between the two areas biased for each polarity in Fig. 3 supports the reliability of the method. Increasing the applied voltage by 0.2 V in the positive polarity results in a corresponding increase in the amount of oxygen exchange between the electrode and oxide. For the positive polarity, the measured currents were close to the target currents of 100 and 250 pA. However, in the negative polarity, the CAFM was unable to induce the target current due to frequently reaching its maximum applied voltage (−10 V). It appears that the redox reaction more readily proceeds in the positive polarity, where oxygen moves from MoO_x to SiO_x. We believe that this asymmetry in the oxygen diffusion is a result of SiO_x having an almost 200 kJ mol^{-1} lower Gibbs free energy of oxide formation than MoO_3. Crucially, this connects the reservoir-like properties of an electrode with the energetics of the materials used. For any ReRAM system, finding an electrode material with an oxide formation energy close to that of the switching layer could improve its reservoir-like properties. This would result in lower energy switching and longer device lifetimes.

The diffusion of oxygen across the ReRAM stack was surprisingly long range, propagating several nanometers, which could be a result of the oxide microstructure. Previous work has shown that our sputtered SiO_x films have a porous, columnar microstructure templated from the sputtered, porous, molybdenum electrode.[10,31] This leads to an interface with a porosity correlated with roughness. Devices with a rougher interface exhibit better and more reliable switching behavior.[31] The rough interfaces in these devices may contribute to oxygen diffusion, observed here, into the molybdenum electrode. Attempts to repeat this experiment for a platinum bottom electrode were unsuccessful due to large changes in the volume of the biased regions. We believe that this is a consequence of the delamination described above, supporting the ineffectiveness of platinum as an oxygen reservoir. For this platinum device, the material changes were too great to be able to reliably compare regions side by side. This shows a limitation of our SIMS method. However, this limitation only appears when devices undergo large deformations and start to break down. Our measurements here show that a device that performs well has a significant and reversible exchange of oxygen with the lower electrode. Crucially, our method can measure and compare this oxygen diffusion. Looking at other electrodes, we can measure the impact of Gibbs free energies of oxide formation and microstructure on oxygen diffusion. This should enable us to maximize oxygen exchange and further improve performance.

Figure 3 also shows that under a negative tip bias (blue), there is a >10% increase in oxygen concentration near the surface of SiO_x. This reveals interaction with the ambient environment, more specifically moisture. However, before discussing this, it is first important to look at the electric field distribution in our system. We used Comsol to model the electrical fields present for a device under operation in ambient moisture. Simulations have previously shown that rough interfaces produce local field enhancements.[32] In order to take account of this, we generated a model that used real measurements of interface roughness and porosity derived from AFM mapping and SEM micrographs, respectively, of our devices. TEM micrographs have previously been used to fit the interface roughness; however, this is the first time, to our knowledge, that porosity has also been considered in such simulations.[33] Crucially, ambient moisture was assumed to penetrate the pores and form a meniscus at the edges of the electrode, as it would in an operating device. The corresponding electric fields during biasing for an ReRAM device with a top electrode at −5 V are illustrated in Fig. 4(a) and for a biased CAFM tip in Fig. 4(b). Both have comparable field strengths and gradients in the moisture and switching layer. We can therefore be confident that the changes under biasing with a CAFM tip are representative of a device with a top electrode. The system was modeled with a 1.5 nm water gap between the CAFM tip and SiO_x surface as the force applied to the tip was estimated to be 6 nN, which is insufficient to break through an aqueous layer.[35,36] The fields induced in the moisture at the surface of the switching layer considerably surpass the breakdown field of water, which is in the range of 0.2–0.75 MV/cm.[37,38] Hence, under a negative top electrode bias, the field-induced breakdown of moisture will generate O- and OH-ions, which will be driven into the switching layer. This process is already used for nano-patterning substrates with an AFM tip through anodic oxidation.[38] These simulations show us how the same mechanism can be responsible for introducing moisture into resistance switching devices through electrode pores and edges. This will likely also result in the introduction of hydrogen into the system, which can also influence conductivity.[39] ^{18}O tracers have previously been used to demonstrate this moisture injection into the switching layer during operation, though the mechanism remains contentious.[18] In our simulation, the field strength is enhanced at the pores—where moisture is present. As these points of enhancement are where electroforming is expected to occur, ambient moisture is present at the points of greatest material change.

In the next experiment, three devices were fabricated to investigate the influence of the materials system on the injection of oxygen into the surface of SiO_x from the ambient. The same conditions were used to sputter deposit 12 nm of SiO_x onto three different electrodes. X-ray photoelectron spectroscopy confirmed the O/Si stoichiometry in the SiO_x films varied by under 2.5% between devices. The three electrodes used were: sputtered Mo (from Fig. 3), sputtered Ti, and evaporated Pt. The surface roughness of the electrodes decreased in that order. The SEM micrographs of the oxide surface show a corresponding decrease in porosity as the bottom electrode roughness is reduced (Fig. 5: right). This variation in the microstructure is a result of shadowing from the bottom electrode, which influences the growth of the sputtered SiO_x film.[31,41] CAFM biasing of areas was carried out on the three devices. After biasing, the areas' SIMS depth profiles were taken and *in situ* normalization was applied, as in Fig. 3. The results are shown in Fig. 5 with the average voltage and currents applied labeled for each area.

The SIMS depth profile in Fig. 5(a) shows a clear increase in oxygen concentration at the surface of SiO_x. Considering a negative tip bias will drive negative oxygen ions from the top surface of the oxide toward the bottom electrode (i.e., from left to right Fig. 5), this oxygen must have come from the environment, likely from ambient moisture. From panels (a)–(c), there is a general trend of a reduction in the oxygen injection. Although for (a) and (c) the trend is clear, the fluctuation in (b) is more complicated. It appears that as well as

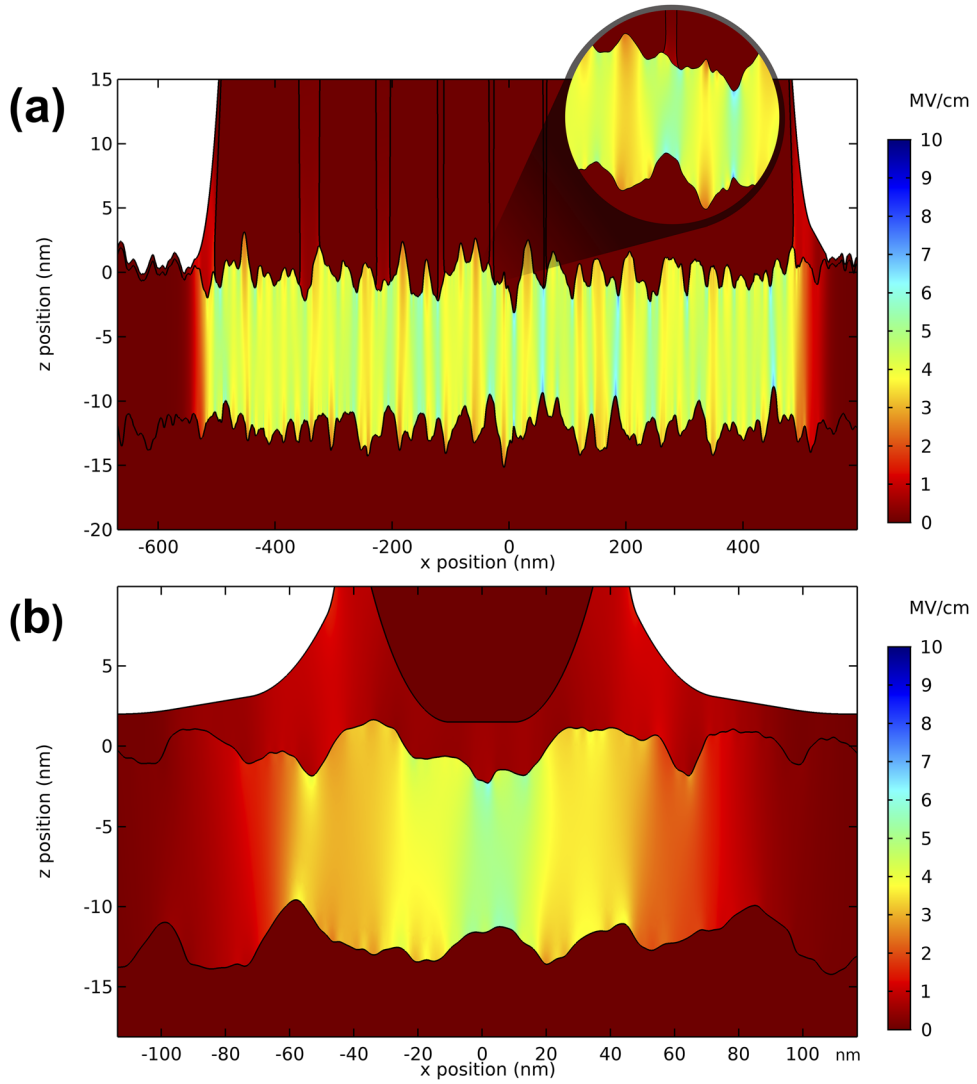

FIG. 4. Comsol modeling of the electric field present. (a) Porous RERAM device with open vertical channels through the electrode of varying size. Moisture is fitted to permeate the channels and form a meniscus at the edge of the electrode. Inset: Region below one of the pores. (b) CAFM probe in surface water also fitted with a water meniscus showing comparable field strengths and distributions to (a).

injection from the ambient, oxygen already present in the oxide is also moving under the applied field although this is not fully understood. However, as with the other areas, there is a strong consistency between the SIMS measurements from the two biased areas, which suggests that the results in (b) are not an artifact. This demonstrates that this measurement technique can effectively track the complex dynamics in these systems.

There are three main factors that could be contributing to the changes in oxygen injection at the surface of SiO_x for the three devices. The first factor is the change in the applied field. SiO_x was 12 nm thick for all three devices, so the field across the oxide is proportional to the applied voltage. As oxygen diffusion is field driven, the change in the voltage applied to the devices will undoubtedly influence the amount of oxygen injected at the surface. The intention of using target currents of 100 and 250 pA was to increase the average applied voltage, and hence field, measuring its influence on the injection of oxygen. Although the voltages for the two target currents vary only slightly, they give some indication of the effects of field—in general, a higher field results in greater changes in the oxide, as expected. However, there is a measurement with an applied voltage greater than −9 V for all three devices. At this higher voltage, there were still large differences in the oxygen injection, which mean that it is unlikely that the changes between devices were a product of the field. The second factor is the bottom electrode material, which changed between devices, which could change device resistance through interface oxidation. A higher resistance at

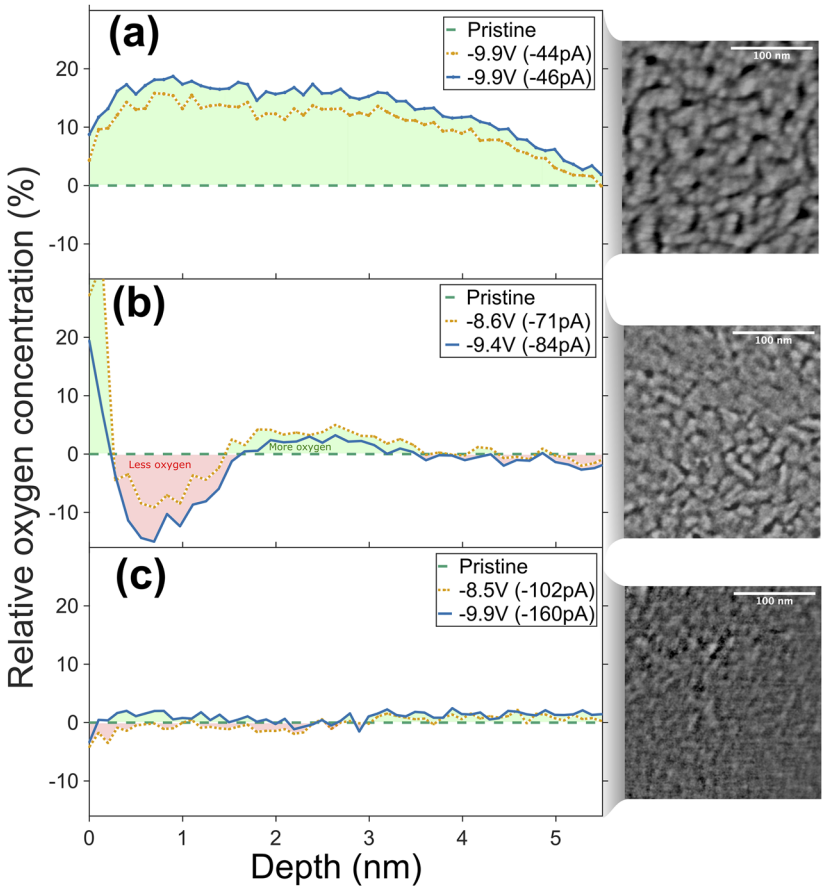

FIG. 5. Analysis of three SiO_x samples with different porosities. Right: SEM images of the SiO_x surface for three samples of decreasing porosity. Left: Normalized SIMS depth profiles of oxygen concentration from the surface to bulk of the SiOx layer. The measured average voltages and currents applied to each area with the CAFM are displayed in the key. As the porosity of the sample decreases, the range and amount of oxygen injected from the environment also decrease.

the interface could reduce the proportion of the voltage, and hence field, across SiO_x. However, for a comparable applied voltage, there is an inverse relationship between the average current and oxygen injection into devices. Therefore, the effect of the bottom electrode material does not appear to be significant. This leaves one significant difference between the device: microstructure. We hypothesized that changes in the microstructure would influence the injection of moisture at the SiO_x surface. While this has not received much attention in the literature, differences in the microstructure will lead to very different interaction surfaces. The average pore size decreases by approximately a factor of two from (a) to (b); at (c), the microstructure becomes almost undetectable. With the reduction in the oxide porosity, there is a strong corresponding reduction in the oxygen injection. For (c), there appears to be such a fine microstructure that the injection of oxygen is prevented entirely.

These results have two key implications. First, they provide empirical evidence of moisture injection into devices. Second, they directly link the amount of oxygen injected from ambient moisture to the microstructure of the oxide layer. Therefore, we have an experimentally confirmed means by which moisture injection into devices can be measured and controlled—changing the oxide porosity. Our SIMS *in situ* normalization allows us to compare different materials systems measuring small changes in ion diffusion, which is a step toward designing better devices.

III. CONCLUSION

We have developed a powerful new SIMS analysis method for measuring chemical changes across switching layers and electrodes. We can measure bulk concentration changes in a continuous profile with unprecedented sensitivity. Applying this to ReRAM devices reveals several features that were previously unobservable due to instrumental limitations. We have demonstrated the oxygen reservoir-like behavior of a molybdenum electrode, exchanging oxygen with SiO_x under opposite biases. This exchange appears to be crucial to device operation and, when prevented, leads to delamination and device failure. Our results indicate that tuning the energetics and microstructure of the electrodes can improve this exchange and thus produce more reliable devices with longer lifetimes. Looking at the relationship between the SiO_x microstructure and the devices' interaction with ambient moisture, we find that increased porosity leads to the greater injection of oxygen from the ambient. Again, this provides a means by which devices can be improved: The SiO_x microstructure can be tuned to control the influence of ambient moisture. Modeling of the electric fields present in our devices during operation helps to support and explain these findings, showing that the field-induced breakdown of moisture can generate oxidative ions and drive them into devices through pores in the electrodes. Although we demonstrate this for SiO_x devices, our results

are broadly applicable to any device with a rough interface that may host oxygen exchange. The oxygen reservoirs and microstructure appear to be crucial to resistance switching performance. Looking forward, this method could be used on more powerful SIMS instrumentation and extended to look at the diffusion of other ions, such as hydrogen and other impurities. This work and the method developed could provide an elusive key to understanding and addressing problems with ReRAM device reliability. In turn, this will enable the improvements required to implement novel non-volatile memory devices and brain-inspired functional units, potentially transforming the way we store and compute for a new generation of computing hardware for artificial intelligence.

IV. EXPERIMENTAL METHODS

The SiO_x ReRAM devices discussed in this work were deposited on a *p*-type silicon wafer covered with a 1 μm electrically isolating layer of thermally grown SiO_2.

The Mo and Ti electrodes were deposited by sputtering in an argon environment, and the Pt electrode was deposited by thermal evaporation. The SiO_x layer was deposited by reactive sputtering using a silicon target in an argon and oxygen environment. This produced a sub-stoichiometric, silicon-rich film with $x \approx 1.7$ (confirmed by x-ray photoelectron spectroscopy[41]). SEM micrographs of the oxide surfaces were taken using a Zeiss Auriga Cross beam instrument with a spatial resolution of 1 nm. CAFM electrical stressing of sample regions was carried out with a Bruker Icon microscope, using solid platinum probes. The deflection sensitivity of the setup was 100 nm/V, and we applied a deflection setpoint of 0.2 V. This gives an estimated applied force of 6 nN. Scanning was performed in the constant-current mode with a tip velocity of 10 μm s^{-1}. First, the target current was set, and then the voltage range was increased from 0 to ±10 V at around 1 V s^{-1}, with the tip height held constant. For all scans, the tip was grounded and the bias was applied to the stage, which was connected to the bottom electrode of the sample with a metal clip. The biased regions were subsequently analyzed using an ION-TOF TOF-SIMS V instrument. The depth profiles were generated by sputtering samples with a 1 keV, 70 nA Cs^+ beam and using a 25 keV Bi^+ analytical ion beam for secondary ion generation. Charge compensation was performed using a low energy electron gun. To isolate the changes induced by biasing, point to point normalization was carried out between biased and pristine regions using MATLAB.

ACKNOWLEDGMENTS

We would like to gratefully acknowledge funding from the EPSRC (Grant No. EP/P013503/1) "Structural dynamics of amorphous functional oxides—the role of morphology and electrical stress." H.R.J.C. gratefully acknowledges funding from the EPSRC and SFI Centre for Doctoral Training in Advanced Characterisation of Materials (Grant No. EP/L015277/1). A.M. would like to acknowledge the Royal Academy of Engineering and the support through the research fellowship.

AUTHOR DECLARATIONS

Conflict of Interest

The authors have no conflicts to disclose.

DATA AVAILABILITY

The data that support the findings of this study are available from the corresponding author upon reasonable request.

REFERENCES

[1] D. I. Son, J. H. Shim, D. H. Park, J. H. Jung, J. M. Lee, W. Il Park, T. W. Kim, and W. K. Choi, Nanotechnology **22**, 295203 (2011).
[2] M.-J. Lee, C. B. Lee, D. Lee, S. R. Lee, M. Chang, J. H. Hur, Y.-B. Kim, C.-J. Kim, D. H. Seo, S. Seo, U.-I. Chung, I.-K. Yoo, and K. Kim, Nat. Mater. **10**, 625 (2011).
[3] A. Mehonic, M. Buckwell, L. Montesi, L. Garnett, S. Hudziak, S. Fearn, R. Chater, D. McPhail, and A. J. Kenyon, J. Appl. Phys. **117**, 124505 (2015).
[4] A. Mehonic and A. J. Kenyon, *Defects at Oxide Surfaces* (Springer International Publishing, 2015).
[5] M. Lübben, S. Wiefels, R. Waser, and I. Valov, Adv. Electron. Mater. **4**, 1700458 (2018).
[6] T. Tsuruoka, K. Terabe, T. Hasegawa, I. Valov, R. Waser, and M. Aono, Adv. Funct. Mater. **22**, 70 (2012).
[7] J. S. Lee, S. Lee, and T. W. Noh, Appl. Phys. Rev. **2**, 031303 (2015).
[8] D. Cooper, C. Baeumer, N. Bernier, A. Marchewka, C. La Torre, R. E. Dunin-Borkowski, S. Menzel, R. Waser, and R. Dittmann, Adv. Mater. **29**, 1700212 (2017).
[9] G. S. Park, Y. B. Kim, S. Y. Park, X. S. Li, S. Heo, M. J. Lee, M. Chang, J. H. Kwon, M. Kim, U. I. Chung, R. Dittmann, R. Waser, and K. Kim, Nat. Commun. **4**, 2382 (2013).
[10] A. Mehonic, M. Buckwell, L. Montesi, M. S. Munde, D. Gao, S. Hudziak, R. J. Chater, S. Fearn, D. McPhail, M. Bosman, A. L. Shluger, and A. J. Kenyon, Adv. Mater. **28**, 7486 (2016).
[11] S. Fearn, *An Introduction to Time-of-Flight Secondary Ion Mass Spectrometry (ToF-SIMS) and its Application to Materials Science* (Morgan & Claypool Publishers, 2015).
[12] H. Téllez, A. Aguadero, J. Druce, M. Burriel, S. Fearn, T. Ishihara, D. S. McPhail, and J. A. Kilner, J. Anal. At. Spectrom. **29**, 1361 (2014).
[13] A. G. Shard, S. J. Spencer, S. A. Smith, R. Havelund, and I. S. Gilmore, Int. J. Mass Spectrom. **377**, 599 (2015).
[14] M. Lorenz, D. Hirsch, C. Patzig, T. Höche, S. Hohenberger, H. Hochmuth, V. Lazenka, K. Temst, and M. Grundmann, ACS Appl. Mater. Interfaces **9**, 18956 (2017).
[15] C.-Y. Lin, D.-Y. Lee, S.-Y. Wang, C.-C. Lin, and T.-Y. Tseng, Surf. Coat. Technol. **203**, 628 (2008).
[16] K. L. Lin, T. H. Hou, J. Shieh, J. H. Lin, C. T. Chou, and Y. J. Lee, J. Appl. Phys. **109**, 084104 (2011).
[17] K. L. Lin, T. H. Hou, Y. J. Lee, J. W. Chang, J. H. Lin, J. Shieh, C. T. Chou, T. F. Lei, W. H. Chang, W. Y. Jang, and C. H. Lin, Jpn. J. Appl. Phys., Part 1 **52**, 031801 (2013).
[18] T. Heisig, C. Baeumer, U. N. Gries, M. P. Mueller, C. La Torre, M. Luebben, N. Raab, H. Du, S. Menzel, D. N. Mueller, C. L. Jia, J. Mayer, R. Waser, I. Valov, R. A. De Souza, and R. Dittmann, Adv. Mater. **30**, 1800957 (2018).
[19] C. Yoshida, K. Kinoshita, T. Yamasaki, and Y. Sugiyama, Appl. Phys. Lett. **93**, 042106 (2008).
[20] M. Buckwell, W. H. Ng, D. J. Mannion, S. Hudziak, A. Mehonic, and A. J. Kenyon, arXiv:2010.15184 (2020).
[21] D. S. McPhail, J. Mater. Sci. **41**, 873 (2006).
[22] D. P. Chu and M. G. Dowsett, Phys. Rev. B **56**, 15167 (1997).
[23] S. Kim, H. J. Jung, J. C. Kim, K.-S. Lee, S. S. Park, V. P. Dravid, K. He, and H. Y. Jeong, ACS Nano **12**, 7335 (2018).
[24] K. Szot, W. Speier, G. Bihlmayer, and R. Waser, Nat. Mater. **5**, 312 (2006).
[25] A. Mehonic, A. L. Shluger, D. Gao, I. Valov, E. Miranda, D. Ielmini, A. Bricalli, E. Ambrosi, C. Li, J. J. Yang, Q. Xia, and A. J. Kenyon, Adv. Mater. **30**, 1801187 (2018).

[26]J. R. Rumble, *CRC Handbook of Chemistry and Physics*, 101st ed. (CRC Press, 2020).
[27]T. Bertaud, M. Sowinska, D. Walczyk, S. Thiess, A. Gloskovskii, C. Walczyk, and T. Schroeder, Appl. Phys. Lett. **101**, 143501 (2012).
[28]N. Xu, L. F. Liu, X. Sun, C. Chen, Y. Wang, D. D. Han, X. Y. Liu, R. Q. Han, J. F. Kang, and B. Yu, Semicond. Sci. Technol. **23**, 075019 (2008).
[29]W.-Y. Chang, H.-W. Huang, W.-T. Wang, C.-H. Hou, Y.-L. Chueh, and J.-H. He, J. Electrochem. Soc. **159**, G29 (2012).
[30]A. J. Kenyon, M. Singh Munde, W. H. Ng, M. Buckwell, D. Joksas, and A. Mehonic, Faraday Discuss. **213**, 151 (2019).
[31]M. S. Munde, A. Mehonic, W. H. Ng, M. Buckwell, L. Montesi, M. Bosman, A. L. Shluger, and A. J. Kenyon, Sci. Rep. **7**, 9274 (2017).
[32]S. K. Nandi, X. Liu, D. K. Venkatachalam, and R. G. Elliman, Phys. Rev. Appl. **4**, 064010 (2015).
[33]N. Gaillard, L. Pinzelli, M. Gros-Jean, and A. Bsiesy, Appl. Phys. Lett. **89**, 133506 (2006).
[34]L. Jiang, J. Weber, F. M. Puglisi, P. Pavan, L. Larcher, W. Frammelsberger, G. Benstetter, and M. Lanza, Materials **12**, 459 (2019).
[35]G. Benstetter, A. Hofer, D. Liu, W. Frammelsberger, and M. Lanza, *Conductive Atomic Force Microscopy: Applications in Nanomaterials* (Wiley VCH, 2017).
[36]H. M. Jones and E. E. Kunhardt, J. Phys. D: Appl. Phys. **28**, 178 (1995).
[37]S. Thivya and V. Gowri Sree, *Proceedings of 13th IRF International Conference, Bengaluru, India, 24 May 2015* (IRF, 2015).
[38]M. H. Lee and C. S. Hwang, Nanoscale **3**, 490 (2011).
[39]H. Noh, J. Kim, J.-S. Kim, M.-J. Lee, and H.-J. Lee, Crystals **9**, 75 (2019).
[40]J. F. Whitacre, Z. U. Rek, J. C. Bilello, and S. M. Yalisove, J. Appl. Phys. **84**, 1346 (1998).
[41]A. Mehonic, M. S. Munde, W. H. Ng, M. Buckwell, L. Montesi, M. Bosman, A. L. Shluger, and A. J. Kenyon, Microelectron. Eng. **178**, 98 (2017).